Combined Raman and Computational Study of a Novel Series of Macrocyclic π-Conjugated Diacetylene-Bridged α-Linked Oligothiophenes

M. C. Ruiz Delgado,[†] J. Casado,[†] V. Hernandez,[†] J. T. Lopez Navarrete,*[,†] G. Fuhrmann,[‡] and P. Bäuerle*[,‡]

Departamento de Química Física, Facultad de Ciencias, Universidad de Málaga, 29071 Málaga, Spain, and Department of Organic Chemistry II (Organic Materials and Combinatorial Chemistry), University of Ulm, Albert-Einstein-Allee 11, D-89081 Ulm, Germany

Received: October 2, 2003; In Final Form: January 9, 2004

We present here a Raman study of a series of macrocyclic molecular materials containing various symmetrically butylated terthienyl or quinquethienyl segments connected through diacetylenic bridges, in the neutral state as solids. Comparison of the Raman features of the macrocycles with those of various linear diacetylenic-bridged oligothiophenes of short chain lengths suggests the coexistence in the macrocycles of different molecular conformations. In particular, Raman bands around 2180 cm^{-1} (due to the diacetylenic bridges) and in the 1550−1450 cm^{-1} region (due to the aromatic C═C stretchings) of the macrocycles are broader than those of the linear compounds, as a consequence of frequencies and intensity changes on cyclization, which qualify them as structure-sensitive marker bands. In addition, these Raman bands undergo frequency downshifts on going from −170 to +160 °C, which is also consistent with conformational changes of low energy. This thermal study reveals, at the molecular level, that the compounds studied are stable between −170 and +160 °C, which is important for their practical use in technological applications. DFT and HF molecular geometries and vibrational calculations on suitable models indicate that the rotation of two oligothienyl segments around a central diacetylenic bridge induces almost negligible changes either in the skeletal bond distances or in the Raman scattering profile, thus not affecting the degree of π conjugation of the macrocycle. This result is clearly attributable to the cylindrical symmetry of the diacetylenic spacer. On the other hand, calculations performed for different molecular arrangements of the thienyl units along a given oligothienyl brick predict higher spectral changes, in agreement with what is actually found. Nonetheless, the overall π conjugation of the macrocycles seems to have very little dependence on the molecular conformation and to be primarily determined by the number of building blocks and the chain length of the oligothienyl segments.

Introduction

Polythiophenes and their finite model oligomers, α-oligothiophenes, belong to the most thoroughly investigated π-conjugated systems due to the chemical stability of their various redox forms, their outstanding electronic properties, the widespread possibilities of functionalization, and their potential applicability in a great variety of molecular electronic devices such as organic light emitting diodes, transistors, and lasers.[1] The analysis of many series of monodisperse linear α-linked oligothiophenes with defined chemical structures has demonstrated that the trend of variation of the relevant physical properties correlate well with the conjugated chain length, and thus, the structure−property relationships become, in this way, easily accessible.[2]

Well-defined π-conjugated macrocycles are the subject of great current interest as modular building blocks for the programmed assembly on new molecular materials[3] and supramolecular nanoscale architectures,[4] and not only because of their higher molecular symmetry. If the macrocyclic systems were sufficiently stable and large, in comparison to usual linear π-conjugated oligomers and polymers, completely novel perspectives and properties could arise. For example, macrocyclic derivatives could represent a model system which ideally combines an infinite π-conjugated path of an idealized polymer with the advantages of a structurally well-defined oligomer lacking of any perturbing end-effect.[5] In this respect, and due to their toroidal structure, they could act as intriguing "molecular circuits" which would additionally include sites, as a consequence of the resulting cavities, for the recognition and selective complexation of guest molecules, depending on the redox state of the macrocyclic host. On the other hand, some types of macrocycles such as cyclic oligopeptides can self-assemble to form nanotubes, enabling their application in biological as well as materials science.[6]

Some of us have recently reported the successful synthesis of the first series of fully π-conjugated macrocyclic toroidal structures in which symmetrically butylated terthiophene or quinquethiophene building blocks are connected through diacetylenic bridges.[7] The most interesting adsorption and self-assembly properties of these novel macrocyclic oligothiophene-diacetylenes have also been studied by in situ scanning tunneling microscopy (STM) at the solution/HOPG (high oriented pyrolythic graphite) interface.[8]

Raman spectra of polyconjugated compounds show unusual features directly related to the degree of π-electron delocalization in neutral state and to the charged carriers created upon doping or photoexcitation.[9−13] In addition, it is hard to assess detailed structural information on a doped material in terms of bond

* To whom correspondence should be addressed. (J.T.L.N.) E-mail: teodomiro@uma.es. (P.B.) E-mail: peter.baeuerle@chemie.uni-ulm.de.
[†] Universidad de Málaga.
[‡] University of Ulm.

10.1021/jp036956o CCC: $27.50
Published on Web 02/13/2004

lengths and angles by means of many usual experimental techniques. However, the combination of quantum-chemical calculations with vibrational spectroscopic data provides a very valuable source of structural information. In fact, this type of study is among the most powerful tools to prove, on a molecular scale, the electronic and structural modifications taking place in a material upon chemical or electrochemical doping.[11,12]

The aim of the present work is to analyze at the molecular level, by combining Fourier transform Raman (FT-Raman) spectroscopy with quantum chemical calculations, the efficiency of the π conjugations in the above class of macrocyclic oligothiophene−diacetylenes, in the neutral state as solids. The Raman features of the macrocycles will be compared with those of open-chain model systems built up from two α-linked oligothiophene end moieties (i.e., terthiophene or quinquethiophene) attached to a central diacetylenic spacer with the aim of deriving information about the dependence of the π conjugation of these macrocycles either with increasing length of the oligothiophene moieties or with increasing number of building blocks in the macrocycle. The thermal stability of the macrocycles in the neutral state will be also experimentally studied by recording Raman spectra at different temperatures between −170 and +160 °C.

Experimental and Computational Details

The synthesis of the fully α-conjugated macrocyclic oligothiophenes studied in this work has been reported elsewhere[7] (chemical structures of the cyclic and open chain compounds to be studied along the paper are depicted in Figure 1, together with the abbreviated nominations to be used throughout the text).

FT-Raman spectra were collected with the FT-Raman accessory kit (FRA/106-S) of a Bruker Equinox 55 FT-IR spectrometer. A continuous-wave Nd:YAG laser working at 1064 nm was employed for Raman excitation, with the operating power adjusted to a level lower than 50 mW (to avoid possible damage of the samples upon laser radiation). A germanium photoresistor operating at liquid nitrogen temperature was used as the near-infrared detector. Light reflected and scattered off the samples was filtered to remove that elastically scattered and passed through a Michelson interferometer in a backscattering arrangement. Samples were analyzed in the form of solids in sealed capillaries. Typically, 1000 scans with a spectral resolution of 2 cm^{-1} were averaged in all Raman experiments to optimize the signal-to-noise ratio.

A variable temperature cell Specac P/N 21525, with quartz windows, was used to record the FT-Raman spectra at different temperatures. The cell consists of a surrounding vacuum jacket (0.5 Torr), which contains a combination of a refrigerant dewar and a heating block as the sample holder. It was also equipped with a Copper−Constantan thermocouple for temperature monitoring purposes, and any temperature from −190 to +250 °C (83−523 K) can be achieved. Pure solids were inserted into the heating block of the sample holder in the form of KBr pellets. Spectra were recorded after waiting for thermal equilibrium at the sample, which required 20 min for every increment of 10 °C.

Density functional theory (DFT) and Hartree−Fock (HF) calculations were carried out by means of the Gaussian 98 program[14] running on a SGI Origin 2000 computer. As for DFT, we used the Becke's three-parameter exchange functional combined with the LYP correlation functional (B3LYP).[15] It has already been shown that the B3LYP functional yields similar geometries for medium-sized molecules as MP2 calculations do with the same basis sets.[16,17] Moreover, DFT force fields calculated using the B3LYP functional yield vibrational spectra in very good agreement with experiments.[18,19] We made use, both for the DFT and HF methodologies, of the standard 3-21G* basis set.[20] At this level, the calculated harmonic force constants and vibrational frequencies are usually higher than the corresponding experimental quantities due to a combination of electron correlation effects, basis set defficiencies, and the effect of the anharmonicity. Nonetheless, since the errors in the frequency calculations are largely systematic, they can be corrected after inclusion of appropriate scaling factors. We used the often-practiced adjustment of the theoretical force fields in which frequencies are uniformly scaled down by a factor of 0.98 for the 3-21G* calculations, as recommended by Scott and Radom.[19] This approach is very attractive for large-scale studies because it avoids the fairly complex procedure of defining internal coordinates. The accuracy of the results obtained in this way may be sufficient to disentangle serious experimental misassignments. All quoted vibrational frequencies reported along the paper are thus scaled values. The theoretical spectra were obtaining by convoluting the scaled frequencies with Gaussian functions (10 cm^{-1} width at the half-height). The relative heights of the Gaussians were determined from the theoretical Raman scattering activities.

Due to the large size of the macrocyclic compounds studied in this work, quantum chemical calculations were carried out on two families of model systems: (i) two end-terthienyl moieties attached to a central diacetylenic spacer (i.e., a **3T-DA-3T** model in various molecular conformations) and (ii) a central terthiophene or quinquethiophene backbone with its two end α,α′-positions capped by thienyl-diacetylene moieties (hereafter referred to as **1T-DA-3T-DA-1T** and **1T-DA-5T-DA-1T**, respectively). In the last case, we have also analyzed the effects of the conformational disorder on the Raman spectra by taking into consideration different molecular arrangements of the thienyl units constituting the central quinquethiophene spine.

Results and Discussion

Experimental Raman Spectra. Figure 2 displays the FT−Raman scattering spectra of the neutral forms of the open chain **1T-DA-1T**, **3T-DA-3T** and **5T-DA-5T** compounds. As already found for many other classes of π-conjugated materials, only a very few lines are seen in the spectra despite the huge number of Raman-active normal vibrations predicted by the optical selection rules. The main Raman feature common to all classes of π-conjugated materials is the overwhelming intensity of some of the lines appearing in the ν(C═C) stretching region.[9−13] The enlarged profile of the Raman spectrum of **3T-DA-3T** (Figure 3) illustrates more precisely how, particularly, the C≡C and C═C stretching modes around 2180 and 1550−1400 cm^{-1}, respectively, and the line at 1060 cm^{-1} gain an overwhelming intensity with respect to the remaining Raman-active normal vibrations.

Raman scattering spectra of low band gap π-conjugated polymers and oligomers are usually recorded in full or near-resonance conditions. As resonance is approached, only a few Raman-active normal modes (i.e., those modes having a non−vanishing projection along the deformation coordinate describing the equilibrium geometry changes from the ground to the excited electronic state involved in resonance) should gain appreciable intensity relative to all other Raman-active vibrations.[21] Another point of this statement is that the symmetry point group of the molecule in the excited state determines which symmetry species are selectively enhanced in the Raman spectrum; for instance, when the molecular symmetry does not change from the ground

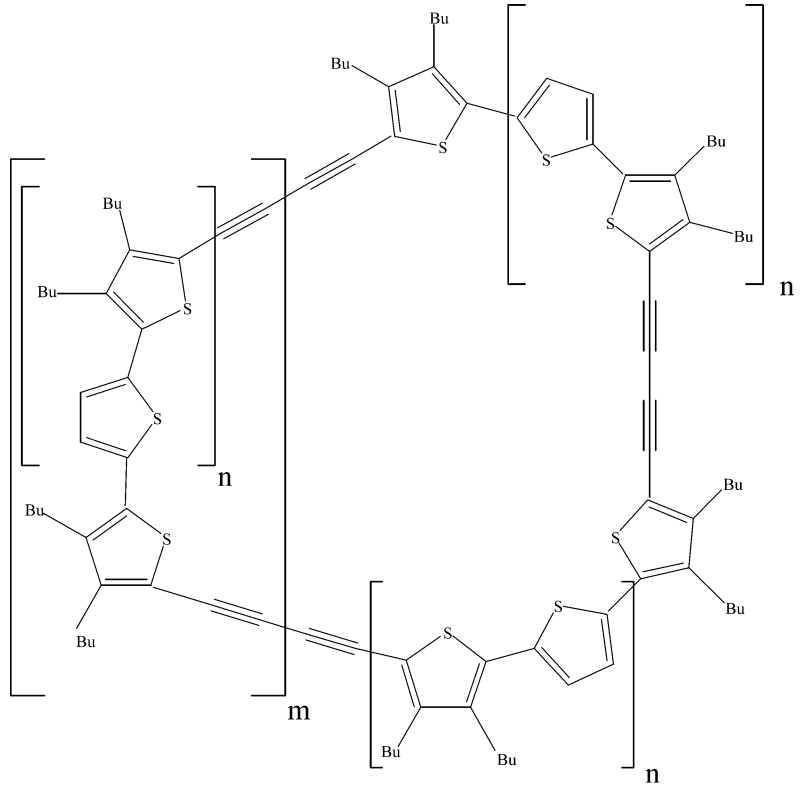

Bu=C_4H_9

C[3T-DA]$_4$; n=1, m=2
C[3T-DA]$_5$; n=1, m=3
C[5T-DA]$_3$; n=2, m=1
C[5T-DA]$_4$; n=2, m=2

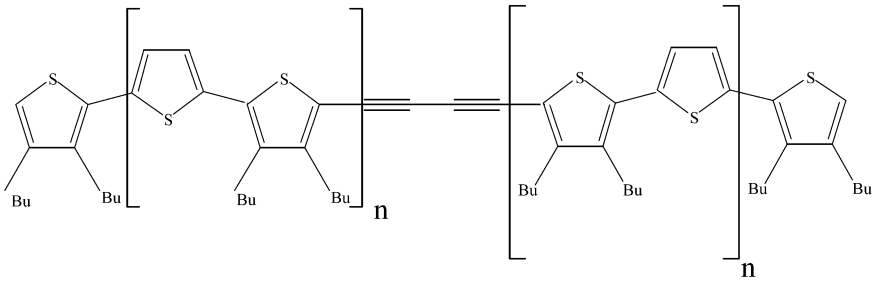

1T-DA-1T; n=0
3T-DA-3T; n=1
5T-DA-5T; n=2

Figure 1. Chemical structures and abbreviatednominations of the open-chain and macrocyclic compounds studied in this work.

to the excited state involved in resonance, only totally symmetric vibrations are enhanced.

However, resonance Raman itself cannot fully account for the spectroscopic behavior of π-conjugated systems. On the contrary, very short conjugated molecules with an energy gap well above the energies of the commonly used optical lasers also show a Raman spectral profile with very few bands;[9−11] whereas FT−Raman spectra collected upon a NIR laser excitation (1064 nm), which is well below the energy gap of the materials under study, show the same spectral pattern as that of the resonant Raman spectra.[11] The key assumption for the adequate interpretation of these intriguing Raman features is that independently that resonance condition is fulfilled or not, only one strong dipole−allowed electronic excited state is relevant for the description of the Raman scattering process in this type of materials (two−state model).[22]

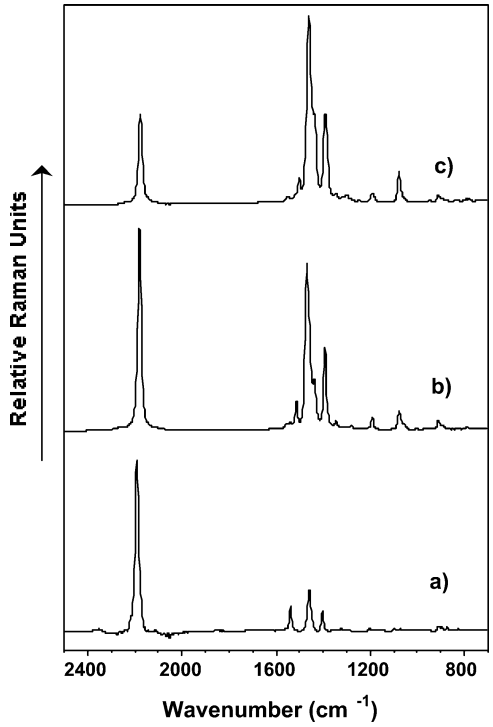

Figure 2. FT-Raman spectra of the neutral forms of (a) **1T-DA-1T**, (b) **3T-DA-3T**, and (c) **5T-DA-5T** open-chain compounds (recorded on pure solids with a laser excitation wavelength of 1064 nm).

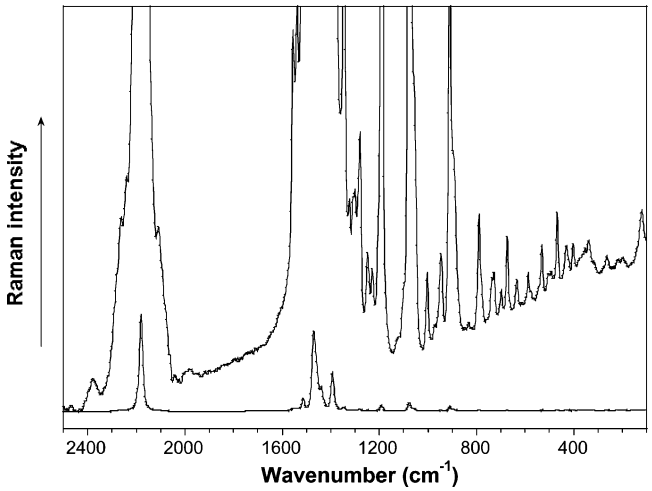

Figure 3. Enlarged profile of the FT-Raman spectrum of **3T-DA-3T**.

At the begining of the scientific research of the π-conjugated polymers, these unusual Raman spectral features attracted the attention of several specialists groups in vibrational spectroscopy. Two main theoretical models were proposed 15 years ago to account for the Raman spectra of π-conjugated materials: (i) the amplitude mode (AM) theory of Horovitz et al.[23] which turned out to be inapplicable to systems with complex chemical structures and (ii) the effective conjugation coordinate (ECC) theory of Zerbi et al.[13] The latter formalism reformulates the concept of *amplitude mode*, first proposed for polyacetylene by Horovitz, in terms of classical molecular dynamics parameters (i.e., internal coordinates and force constants) to account for the Raman spectra of undoped π-conjugated polymers and the infrared spectra of doped and photoexcited polymers.[24−30]

On the basis of the ECC theory,[13] the quite simple Raman spectral profiles of the π-conjugated materials, even for those with very complex molecular structures, result from the existence in this type of systems of a very effective electron−phonon coupling (or electronic delocalization), which extends over the whole π-conjugated backbone. For the aromatic and heteroaromatic π-conjugated systems, the so-called *collective ECC vibrational coordinate* has the analytic form of a linear combination of the ring ν(C═C) and ν(C−C) stretching modes of the π-conjugated backbone, and it mimics the geometrical evolution from the benzenoid structure (usually that of the ground state) to the quinonoid structure (that corresponding to the electronically excited state or the oxidized species). The ECC formalism states that when the conjugation length (CL) increases the totally symmetric normal modes of the neutral system involved in the molecular dynamics of the ECC coordinate (i.e., those giving rise to the very few Raman bands experimentally observed) undergo sizable dispersions both in frequency and intensity. Changes in the peak positions of the Raman bands with increasing chain length allow the effective CL to be estimated along a given series of oligomers. On the other hand, when π-conjugated oligomers and, in particular, α-oligothiophenes become doped (either chemically or electrochemically) or photoexcited, typically, quinonoid-like charged defects are created.[12] These structural modifications also give rise to a significant downshift of the Raman bands associated to the π-conjugated path. The evolution of the Raman spectral profile between the neutral and the different doped states is a useful tool for elucidating the type of charged carriers created upon oxidation or reduction.[9−12]

The FT-Raman spectra of **1T-DA-1T**, **3T-DA-3T**, and **5T-DA-5T** show the typical dependence, common to many other classes of π-conjugated chain compounds, between the frequencies of the ν(CC) stretchings and the number of repeat units; there indeed occurs a significant redshift of some of the ν(C═C) vibrations as the chain grows longer and π-conjugation increases.[9−13] The Raman scattering of **1T-DA-1T** at 2192 cm^{-1}, due to the totally symmetric in-phase ν(C≡C) stretching of the diacetylenic spacer, downshifts by 9 and 15 cm^{-1} on going to **3T-DA-3T** and **5T-DA-5T**, respectively, as a consequence of the softening of the π-conjugated backbone as the number of thienyl units in the chain increases. The bands appearing below 1600 cm^{-1} are related to vibrations of the oligothienyl segments, and they can be assigned taking into consideration some vibrational studies previously performed for various homologous series of linear α-linked oligothiophenes, aided by different quantum chemical approaches (i.e., HF and DFT).[11,30] The Raman line measured at 1539 cm^{-1} in **1T-DA-1T**, 1513 cm^{-1} in **3T-DA-3T**, and 1501 cm^{-1} in **5T-DA-5T** arises from an antisymmetric ν_{asym}(C═C) stretching vibration mostly localized on the outer units of the oligothienyl segments, for which the motions of the symmetry equivalent atoms from their equilibrium positions occur completely in-phase, so that the whole molecular vibration belongs to the totally symmetric species. This Raman line is a characteristic feature of the oligothiophenes, and it shows a sizable dispersion downward as the oligomeric chain grows longer. For instance, the frequency values for a series of α,α′-dimethyl end-capped oligothiophenes previously studied by us are 1560 cm^{-1} (dimer), 1546 cm^{-1} (trimer), 1533 cm^{-1} (tetramer), and 1525 cm^{-1} (pentamer).[11] We have also observed that the peak position of this Raman line for various sexithiophenes having a well-barrier-well electronic structure of general **3T-X-3T** type also varies from one compound to another, depending on the energy gap difference between the central **X** spacer and the two end-terthienyl **3T** moieties (i.e., on the overall π-conjugation of the molecule). In the case of a 1,2-di[5-(2,2′:5′,2″-terthienyl)]ethane,

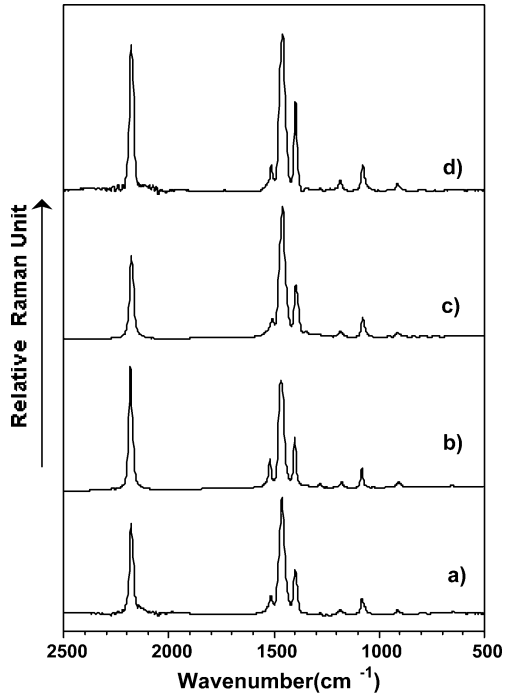

Figure 4. FT-Raman spectra of the neutral forms of the four macrocycles studied in this work (recorded on pure solids with a laser excitation wavelength of 1064 nm); (a) **C[3T-DA]$_5$**, (b) **C[3T-DA]$_4$**, (c) **C[5T-DA]$_4$**, and (d) **C[5T-DA]$_3$**.

3T-Et-3T, this Raman lines was measured at 1535 cm^{-1},[31] whereas it appeared at 1525 cm^{-1} for a 1,2-di[5-(2,2′:5′,2″-terthienyl)]vinylene, **3T-V-3T**.[32] The rather low-frequency value now found for **3T-DA-3T** (1513 cm^{-1}) clearly reflects the sizable involvement of the diacetylene spacer into the overall π-conjugation, and the increased *mean conjugation length* with respect to the other two well-barrier-well sexithiophenes. Moreover, another evidence that the diacetylene group itself is included in the conjugation, and does not act as mere spacer, is shown by the observed Raman lines around 2180 cm^{-1} whereas the corresponding mode in dimethyl diacetylene, for instance, is at 2264 cm^{-1}.

The strong line appearing at 1469 cm^{-1} in **3T-DA-3T** and 1461 cm^{-1} in **5T-DA-5T** arises from a characteristic totally symmetric ν_{sym}(C═C) stretching vibration having a pronounced collective character since it spreads over the whole π-conjugated path of the molecule, and along it all C═C bonds vibrate in-phase and with similar amplitudes. The shoulder appearing near 1438 cm^{-1} at the lower energy side of the latter band is due to a totally symmetric ν_{sym}(C═C) stretching mode, mostly localized on the "bulk" units of the oligothienyl segments, for which the oscillations of the adjacent rings take place in complete out-of-phase. The band at around 1393 cm^{-1} corresponds to the totally symmetric ν(C−C)$_{ring}$ stretching of the aromatic C$_\beta$−C$_\beta$ bonds disubstituted by alkyl side chains (it is absent in all the theoretical Raman spectra reported along this paper since the models lack of alkyl side chains).[33] Finally, the band around 1078 cm^{-1} is due to the totally symmetric δ_{sym}(C$_\beta$−H) in-plane bending mode spreading over all thiophene rings of the π-conjugated backbone, whereas the weak Raman scattering around 1190 cm^{-1} must be assigned to a totally symmetric δ_{sym}-(C$_\beta$−H) in-plane bending mode of the bulk units of the oligothienyl segments, coupled to some extent with ν(C═C)$_{ring}$ stretchings.

The Raman spectral profiles of the macrocycles (see Figure 4) greatly resemble those of the open-chain compounds, the only difference being that the lines at 1513 and 1393 cm^{-1} in **3T-DA-3T** and 1501 and 1391 cm^{-1} in **5T-DA-5T** undergo an upshift of a few cm^{-1} on going from the linear to the cyclic structures.

TABLE 1: Frequencies (in cm^{-1}) Measured for the Main Experimental Raman Lines of the Neutral Forms of the Four Macrocycles Studied in this Work

C[3T-DA]$_4$	C[3T-DA]$_5$	C[5T-DA]$_3$	C[5T-DA]$_4$
2183	2179	2179	2178
1520	1513	1515	1507
1467	1459	1461	1459
1401	1398	1400	1396
1082	1078	1080	1079

The evolution of the experimental Raman features of the macrocycles upon changing either the chain length of the oligothienyl segments or the number of building blocks can also be fully rationalized within the framework of the ECC theory.[13] In particular, we observe that (i) the ν(C═C) stretching at 1467 cm^{-1} becomes stronger than the ν(C≡C) stretching at 2183 cm^{-1} on going from **C[3T-DA]$_4$** to **C[5T-DA]$_4$** (i.e., as the oligothienyl segments become longer), and (ii) all Raman bands appear at lower frequencies with increasing number of building blocks in the macrocycle (Table 1). The main Raman bands experimentally observed for the oligothiophenes are commonly termed as lines A, B, C and D, and their behavior is as follows:

(i) Line A appears above 1500 cm^{-1}. It largely downshifts and weakens (relative to the strongest band around 1460 cm^{-1}) with increasing CL, becoming almost unobservable for relative long chains (i.e., for the octamer).[11,13] As for the cyclic oligothienyl-diacetylenes, line A gives 1520 cm^{-1} **C[3T-DA]$_4$**, 1513 cm^{-1} **C[3T-DA]$_5$** , 1515 cm^{-1} **C[5T-DA]$_3$**, and 1507 cm^{-1} **C[5T-DA]$_4$**. The frequency values are somewhat higher than those observed for the linear **3T-DA-3T** (1513 cm^{-1}) and **5T-DA-5T** (1501 cm^{-1}) compounds. The spectral differences between the macrocycles and the open chain **nT-DA-nT** compounds can be attributed to the changes in the molecular dynamics in going from the *all-anti* to the *all-syn* coplanar configurations of the oligothienyl segments and between oligomeric chains with free and fixed ends. Nonetheless, the characteristic Raman line A appears at frequencies significantly lower than in a homologous series of α,α′-dimethyl end-capped oligothiophenes previously characterized by us.[11] This spectroscopic finding strongly supports the relevant contribution of the diacetylene bridges to the overall π conjugation of the macrocycles.

(ii) Line B is always the strongest band, even for very short chains (i.e., for the trimer). It sizeably downshifts with increasing chain length for the oligopyrroles and oligofuranes but very little for the oligothiophenes, for which it quickly meets saturation.[13,34] Line B undergoes a significant upshift relative to the unsubstituted oligothiophene of the same length upon alkyl-substitution of the end α and/or β positions of the oligothiophene.[9−13] However, along a given series of compounds, it is invariably strong and only slightly shifted from one member to another. For the macrocyclic oligothienyl-diacetylenes, line B is measured at 1467 cm^{-1} **C[3T-DA]$_4$,** 1459 cm^{-1} **C[3T-DA]$_5$** , 1461 cm^{-1} **C[5T-DA]$_3$**, and 1459 cm^{-1} **C[5T-DA]$_4$**, being the frequency values quite close to those found for the unsubstituted oligothiophenes and lower than in the case of the series of α,α′-dimethyl end-capped oligothiophenes.[9,10,13]

(iii) Line C has been clearly observed at the lower energy side of line B only for the α and β-alkyl end-capped oligothiophenes,[11,13] whereas it displays a very weak intensity for the unsubstituted oligothiophenes.[9,10,13] Line C slightly upshifts

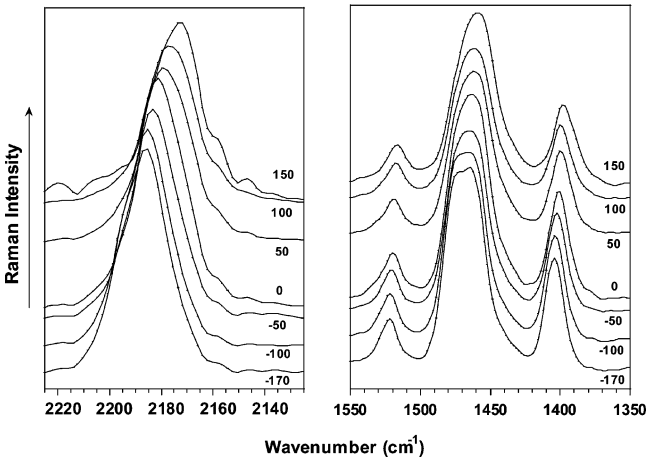

Figure 5. Evolution of the FT-Raman spectrum of **C[3T-DA]$_4$** from −170 to +150 °C, in the 2225−2125 and 1550−1350 cm^{-1} spectral ranges.

and becomes stronger, tending to converge with line B, as the oligothienyl chain grows up.[11] The experimental data so far collected support the hypothesis that the enhancement of line C upon substitution of the outermost thiophene rings of the chain results from a relevant interaction between the π-conjugated spine and the electron-donating end-capping groups.[35] Line C displays a low intensity in the Raman spectra of the macrocycles, which could be attributed to the strong electron-withdrawing character of the diacetylenic bridges connecting the oligothienyl moieties.

(iv) Line D is recorded as a sharp band (sometimes a doublet) of medium-strong intensity at 1050−1080 cm^{-1}. For the macrocycles, line D is measured at 1082 cm^{-1} **C[3T-DA]$_4$**, 1078 cm^{-1} **C[3T-DA]$_5$**, 1080 cm^{-1} **C[5T-DA]$_3$**, and 1079 cm^{-1} **C-[5T-DA]$_4$**.

Finally, we observe that the Raman spectra of **C[3T-DA]$_5$** and **C[5T-DA]$_3$** show a great resemblance, and thus, both macrocycles should display quite similar conjugational properties (a little bit better in the former case as evidenced by the slightly lower frequencies of the related Raman bands, see Table 1). The two macrocycles contain up to 15 thiophene rings, but two additional diacetylenic spacers are present in **C[3T-DA]$_5$**. Despite the little structural difference between the two compounds, FT-Raman spectroscopy proves useful to estimate the efficiency of the π-conjugation.

Thermal Evolution of the Raman Spectra. The variable-temperature FT-Raman spectra of **C[3T-DA]$_4$**, as a prototypical case, are shown in Figure 5. The range of temperatures studied was from −170 to +150 °C (103−423 K); and intermediate points at −100, −50, 0 °C, +50, and +100 °C were also analyzed. The melting point was not reached for any compound. The thermal evolution of the Raman spectrum of **C[3T-DA]$_4$** exhibits rather systematic trends which are common to the four macrocycles studied in this paper. No dramatic changes are noticed before the maximum temperature is reached, and the spectra reversibly recover their profiles throughout the full temperature range examined. A first conclusion is that these molecular materials are thermally stable and do not undergo any undesidered degradation process, at least up to + 150 °C, which has importance for their potential application in technological devices.

The comparison of the spectra of open chain and macrocyclic compounds (Figure 6) shows that the Raman scattering features are broader for the latter systems, as if they were due to an overlap of almost degenerated vibrations (this is particularly evident for the strong scattering around 1460 cm^{-1}). In addition, the infrared absorptions (available upon request to the authors) and Raman bands neither substantially narrow nor split into well-resolved components at low temperatures. We previously found an opposite thermal behavior for a crystalline series of α,α'-dimethyl end-capped oligothiophenes: (i) some infrared bands of the dimer and trimer substantially widened near the melting points of the compounds due to the coexistence of different molecular conformations around the inter-rings C−C bonds and the disappearance of the crystal packing forces, whereas contrarily (ii) a few IR bands clearly resolved into sharp peaks at low temperatures due to the hindered internal rotation and well-ordered intermolecular interactions induced by the close molecular packing.[36]

All of the vibrational spectroscopic information collected as a function of the temperature suggests an amorphous nature for these macrocyclic oligothiophene−diacetylenes, their broad features seemingly arising from the coexistence of different molecular conformations, which however do not substantially affect the overall π conjugation of the system provided that the related enhanced Raman bands of the various conformers appear at quite close frequencies. These observations agree with the theoretical in vacuo "spider-like" molecular shapes, derived from previous semiempirical calculations, with the butyl side chains bent downward, and also with the STM images of the well-ordered and stable self-assembled hexagonal nanoarrays formed by these oligothiophene−diacetylenes at the 1,2,4-trichlorobenzene/HOPG interface.[8]

We have also observed a systematic trend common to many other types of π-conjugated materials, regarding the Raman-active carbon−carbon stretching modes, which supply very useful information about the conjugation length. As discussed in previous papers, along an homogeneous series of π-conjugated oligomers, the frequencies of the ν(C═C) modes shift downward, whereas those of the ν(C−C) modes shift upward when the number of units in the chain increases (i.e., with increasing conjugation length).[9−13] On the other hand, the Raman spectra of the macrocycles collected at increasing temperatures (see Figure 5) also show that the ν(C≡C) and ν(C═C) stretching modes continuosly downshift on going from −170 to +150 °C. Thus, for **C[3T-DA]$_4$**, the totally symmetric ν(C≡C) and the various fully in-phase Raman-active ν(C═C) modes are measured at 2184, 1522, 1474, 1464, and 1404 cm^{-1} (at −170 °C) and at 2173, 1516, 1466, 1459, and 1396 cm^{-1} (at +150 °C), respectively. This thermal Raman dispersion is consistent with the population of conformational states with different π-conjugational properties. In this regard, it can be noticed that the Raman bands of the open chain compounds appear at lower frequencies than those of their related macrocycles (see frequency values in Figure 6). This redshift on going from the toroidal to the linear compounds could be attributed to the molecular dynamics changes between the all-*syn* conformation of the oligothienyl segments (which necessarily must be present in a macrocycle, being likely the main one) to the *all-anti* arrangement of the thiophene rings (i.e., which is commonly found for linear short chain oligothiophenes) or to others in which the thienyl units of a segment were not fully coplanar. The effects of the conformational disorder on the vibrational spectra and molecular geometries will be theoretically investigated along the next section.

Theoretical Calculations for Model Compounds. The chemical structures of the various models to be investigated theoretically are shown in Figure 7, together with the abbreviated nomenclature and bond numberings to be used throughout this

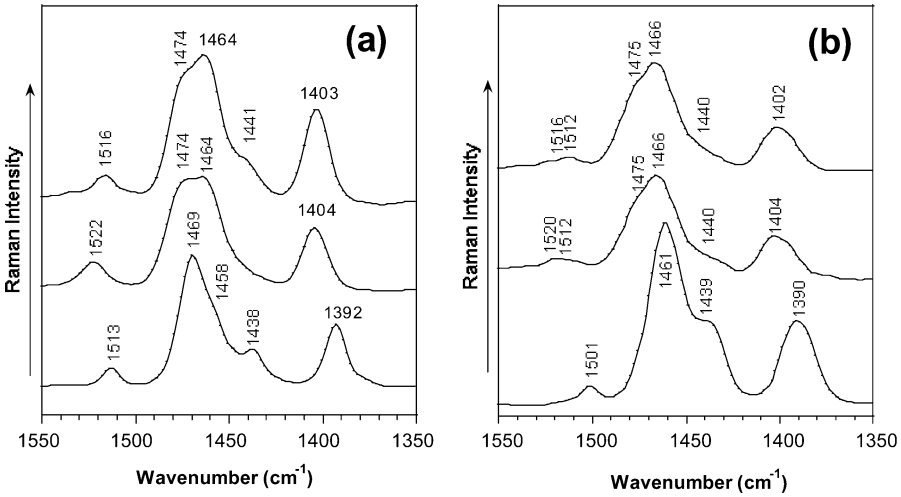

Figure 6. Comparison between the Raman spectra of (a) **3T-DA-3T**, **C[3T-DA]$_4$**, and **C[3T-DA]$_5$** (from bottom to top) and (b) **5T-DA-5T**, **C[5T-DA]$_3$**, and **C[5T-DA]$_4$** (from bottom to top). Spectra of macrocycles correspond to those recorded at −170 °C.

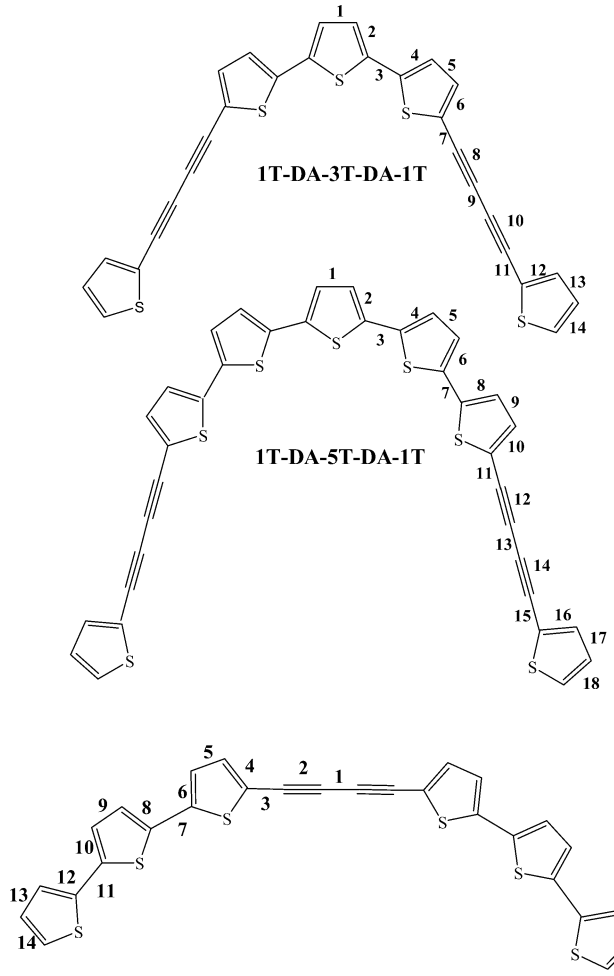

Figure 7. Chemical structures of the model compounds on which theoretical calculations reported throughout the paper were performed (bond numberings are to be used in the tables).

and the next section. We call to the attention of the reader that all models lack of alkyl side-chains to reduce the computational cost. Figure 8 compares the DFT//B3LYP/3-21G* Raman spectrum of **3T-DA-3T** (assuming an *all-anti* configuration of the thiophene units) with the experimental one of the butylated compound. It can be clearly seen that the agreement between theory and experiments is quite satisfactory, being the selective enhancement of the few Raman bands mostly involved in the

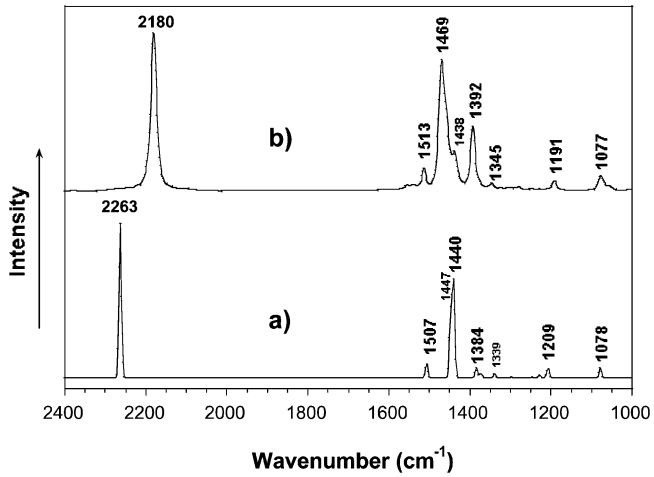

Figure 8. Comparison between the DFT//B3LYP/3-21G* Raman spectrum of **3T-DA-3T** (a) and the experimental one (b).

π-conjugation nicely reproduced both in peak positions and relative intensities. This makes us feel confident about the reliability of the structural information derived from the DFT methodology. Nonetheless, some results will be also obtained by using the RHF methodology and the same 3-21G* basis set. The schematic B3LYP/3-21G* eigenvectors for the main Raman-active normal modes of **3T-DA-3T** (Figure 9) give further suport to the vibrational assignment proposed above.

We have addressed the effect of the conformational disorder on the π conjugation by means of two sets of calculations: (i) in a first step, we assume an *all-syn* conformation for the two terthienyl moieties attached to a central diacetylenic bridge, allowing to vary the dihedral angle defined by their mean least-squares planes, and (ii) second we perform calculations for different molecular conformers of the central quinquethienyl moiety of the **1T-DA-5T-DA-1T** model plotted in Figure 7.

Table 2 reports the optimized CC bond lengths constituting the π-conjugated backbone for three conformers of the **3T-DA-3T** model. Molecular geometries were optimized both at the DFT//B3LYP/3-21G* and RHF/3-21G* levels, with the only constraint of keeping a planar *all-syn* conformation for the two terthienyl end moieties and a fixed dihedral angle between them of $\theta = 0$, 45, and 90°. Bond length differences between the different conformers are lower in any case than 0.001 Å, for both types of calculations, so that the molecular geometry is nearly independent of the possibility of rotation around the

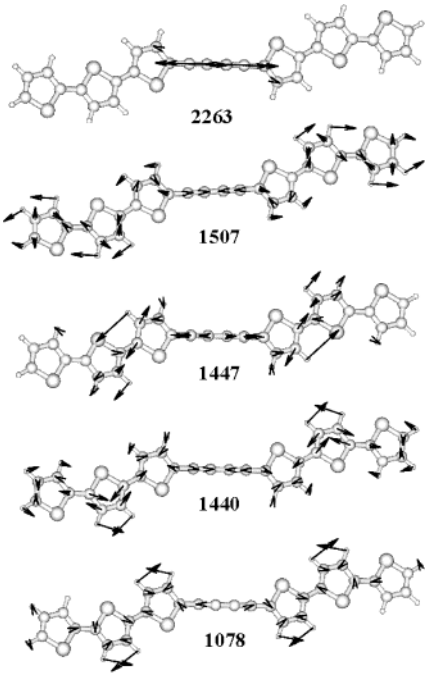

Figure 9. Schematic B3LYP/3-21G* eigenvectors for the main Raman-active normal modes of **3T-DA-3T**.

TABLE 2: B3LYP/3-21G* and RHF/3-21G* Optimized CC Bond Lengths (in Å) for the Three Conformers of 3T−DA−3T Compound[a]

bond no.[b]	B3LYP/3−21G*			RHF/3−21G*		
	$\theta = 0°$	$\theta = 45°$	$\theta = 90°$	$\theta = 0°$	$\theta = 45°$	$\theta = 90°$
1	1.3454	1.3458	1.3461	1.3654	1.3653	1.3652
2	1.2229	1.2229	1.2229	1.1939	1.1940	1.1941
3	1.3922	1.3928	1.3934	1.4105	1.4106	1.4106
4	1.3894	1.3890	1.3884	1.3565	1.3565	1.3564
5	1.4109	1.4110	1.4113	1.4219	1.4217	1.4216
6	1.3892	1.3843	1.3894	1.3593	1.3595	1.3597
7	1.4411	1.4415	1.4420	1.4555	1.4556	1.4556
8	1.3857	1.3855	1.3852	1.3561	1.3561	1.3560
9	1.4149	1.4150	1.4152	1.4240	1.4240	1.4240
10	1.3850	1.3849	1.3849	1.3562	1.3562	1.3562
11	1.4451	1.4453	1.4454	1.4572	1.4572	1.4572
12	1.3832	1.3832	1.3831	1.3560	1.3560	1.3560
13	1.4256	1.4256	1.4257	1.4313	1.4312	1.4312
14	1.3712	1.3712	1.3711	1.3476	1.3476	1.3476

[a] θ is the torsional angle defined by the planes that contain the two terthienyl moieties. [b] Bond numbering is referred to that appearing in Figure 7 for **3T-DA-3T**.

diacetylenic bridge, what is undoubtly related to the cylindric symmetry of its π orbitals. Furthermore, the energy differences between the various conformers studied are lower than 0.5 kcal/mol, meaning that the internal rotation around the DA spacers is scarcely hindered and the torsional potential is rather flat. Finally, we also see that the DFT method predicts a greater contribution from the diacetylene bridge than the RHF methodology to the overall π-conjugation of the system. In this regard, the DFT calculations provide the triple bonds to be longer, by ≈0.03 Å, whereas the CC bond between them being shorter, by ≈0.02 Å, than the RHF values (in the former case, bond number 1 is even predicted to be sizeably shorter than the C═C bonds of the terthienyl moieties). Although DFT methods are known to overestimate the π electrons, the nice resemblance between the experimental Raman profiles and the uniformely scaled down theoretical features aimed us to select this quantum chemical approach as a help for the further analysis of the Raman data collected.

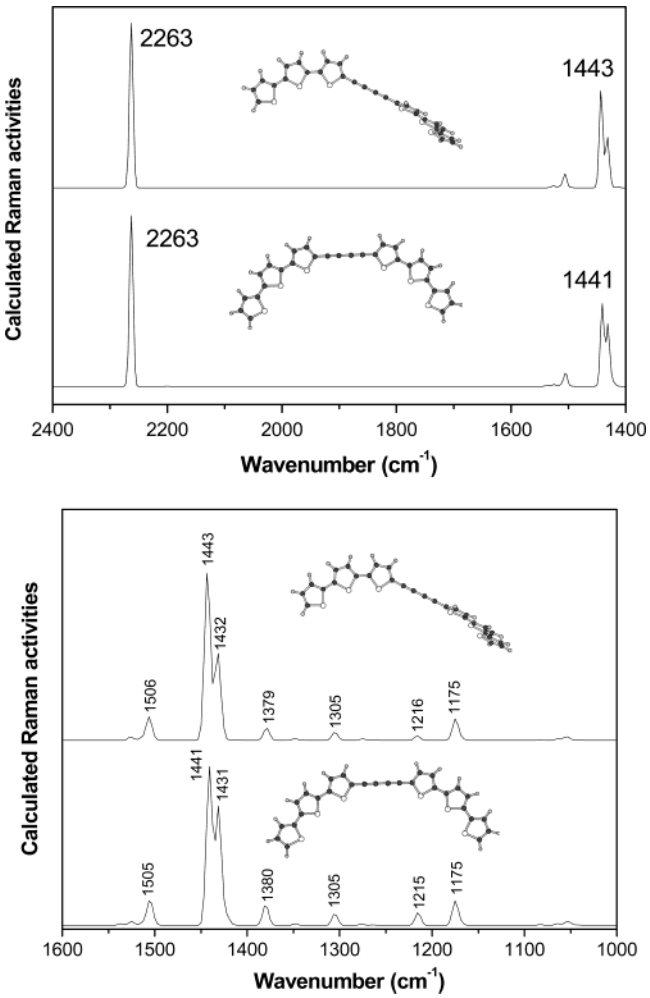

Figure 10. DFT//B3LYP/3-21G* Raman spectra of two different conformers of **3T-DA-3T**.

Figure 10 displays the DFT//B3LYP/3-21G* Raman spectra of the two extreme conformers of **3T-DA-3T** (i.e., the fully coplanar and the perpendicular one). Spectra are fully superposable, so that not only the molecular geometry but also the harmonic force field is almost independent of the rotation around the diacetylene spacers. Conceptually, by changing the conformation of a polyconjugated chain, the changes of the conformationally dependent hopping integrals between the adjacent units should modify the electronic structure, and hence the vibrational force field, and ultimately the vibrational frequencies. As for **3T-DA-3T**, no large variations of the Raman bands are calculated after rotation of the oligothienyl segments. Since the two terthienyl moieties are far apart, it could be argued that no large electronic interactions should take place between them. A key observation is that, even for the perpendicular conformer, the strongest Raman activity at 2263 cm^{-1} (after scaling) still comes from the ν(C≡C) stretching mode and does neither split nor lose intensity with respect to the coplanar conformer. In view of these theoretical results, we can conclude that the π-electrons delocalization through the diacetylenic bridges is quite favored and very little dependent on the mutual orientation of the two oligothiophene moieties.

Since rotation around the diacetylene spacer seems not to be responsible for the observed spectral changes either upon cooling/heating or on going from the open chain to the macrocyclic compounds, we have also analyzed the dependence of the π conjugation on the conformational changes of the thiophene rings along a given oligothiophene segment. With

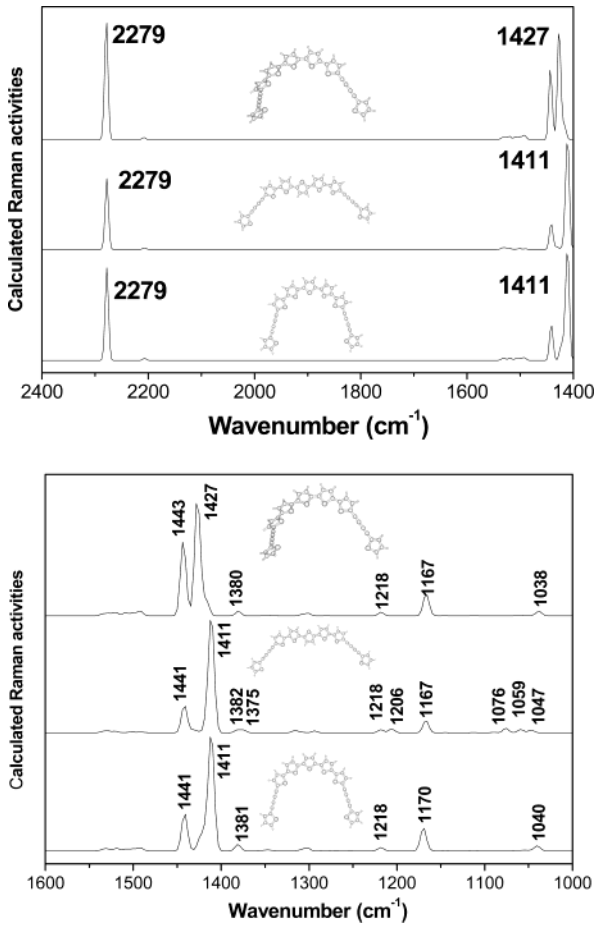

Figure 11. DFT//B3LYP/3-21G* Raman spectra of three different conformers of **1T-DA-5T-DA-1T**.

this purpose, we have taken into consideration three different conformers for the sake of comparison, whose general views together with their DFT//B3LYP/3-21G* Raman spectra are plotted in Figure 11. The lower and middle cases correspond to fully coplanar sequences, whereas the upper case represents a continuous up tilting (each of one by 20°) of the rings of the central quinquethiophene moiety so that the coplanar "U-shaped" model (lower case) evolves into a nonplanar "spiral staircase" structure. No drastic spectral changes are noticed from one model to another. However, going into details, we see that from the *all-syn* "U-shaped" model (lower case) to the coplanar structure containing a central *syn*−*anti*−*syn* "conformational defect" (middle case), a few weak Raman bands (which are however selectively enhanced with respect to the very many Raman-active vibrations) split into different components; in this regard, the single peaks at 1381, 1302, 1218, and 1040 cm^{-1} of the spectrum at the bottom give rise to the doublets at 1382−1375, 1316−1294, and 1218−1206 and the triplet at 1076−1059−1047 cm^{-1} in the spectrum at the middle. On the other hand, on going from the *all-syn* "U-shaped" model (lower case) to the nonplanar "spiral staircase" model (upper case), no splitting is observed but the strong Raman line at 1411 cm^{-1}, which is due to the totally symmetric ν(C═C) stretching commonly known as ECC mode,[13] upshifts by 16 cm^{-1}, and loses some intensity with respect to the Raman ν(C≡C) stretching vibration at 2279 cm^{-1}. The upshift of this Raman line upon loss of coplanarity is clearly related to the less effective overlap between the sp^2 orbital of the carbon atoms at the α positions of the successive thiophene units (so that the overall π conjugation slightly decreases) and could justify for the split into two main bands of the strong Raman scattering of the open-chain **3T-DA-3T** (measured at 1469 cm^{-1}) on going to the macrocycles with terthienyl segments (see Figure 6).

We have only performed calculations on two coplanar quinquethienyl arrangements and one nonplanar sequence with a quite moderate deviation from coplanarity, but even in this case, some spectral differences are expected to occur. It could be reasonably thought that larger conformational distortions than those assumed here for our a nonplanar "spiral staircase" model (of around 20° between each pair of thiophene rings) should translate in more pronounced frequency and intensity changes. At this point, we would like to recall the attention of the reader that our models lack of butyl side-chains; their conformational flexibility should indeed favor the attainment of nonplanar oligothienyl sequences, particularly at high temperatures.

Summary and Conclusions

In this work, we have performed a combined theoretical and vibrational study on a novel series of macrocyclic π-conjugated molecular materials. The compounds contain various oligothienyl segments with their end α positions connected through diacetylene bridges. These toroidal structures can act as guest molecules, and the internal cavity radius can be modulated by changing both the chain length of the oligothienyl moieties or the number of building blocks in the macrocycle. These macrocyclic oligothiophene−diacetylenes display a rather simple Raman spectral profile despite their complex chemical structures, which constitutes a characteristic feature common to many other classes of π-conjugated compounds. The comparison of the frequency and intensity experimental Raman data from one macrocycle to another allows for a estimation of their effective conjugational properties. On the other hand, the comparison of the Raman data of these macrocycles with those of a homologous series of open-chain oligothiophenes intercalated by a central diacetylene spacer reveals a broadening and/or splitting of the stronger scatterings upon cyclization, seemingly due to the coexistence of oligothienyl sequences with different conformations in the same macrocycle. The evolution of the Raman spectra with the temperature gives further support to this hypothesis and in addition reveals that these molecular materials are thermally stable at least up to +150 °C.

Calculations, with the DFT and RHF methodologies, performed on a **3T-DA-3T** model reveals that the rotation of the whole terthienyl end moieties around the central diacetylene spacer does not substantially affect either the molecular geometry or the Raman spectra due to the strong participation of the DA bridge into the overall π conjugation and to its cylindrical symmetry. On the other hand, rotation of the successive units along a given oligothienyl segment translate into small changes in peak positions and relative intensities of the Raman lines, in agreement with what experimentally found. Nonetheless, the effective π-conjugation is almost independent of the molecular conformation of the macrocycle.

Acknowledgment. The authors acknowledge the Dirección General de Enseñanza Superior (DGES, MEC, Spain) for support for this investigation through Projects BQU2000-1156 and BQU2003-3194. The research was also supported by the Junta de Andalucía (Spain), under Grant No. FQM-0159. J.C. is grateful to the Ministerio de Ciencia y Tecnología of Spain for a Ramón y Cajal position of Chemistry at the University of Málaga. M.C.R.D. thanks MEC for a personal grant.

References and Notes

(1) *Handbook of Oligo- and Polythiophenes*; Fichou, D., Ed.; Wiley-VCH: Weinheim, Germany, 1999.

(2) (a) Bäuerle, P. In *Electronic Materials: The Oligomer Approach*; Müllen, K., Wegner, G., Eds.; Wiley-VCH: Weinheim, Germany, 1998. (b) Martin, R. E.; Diederich, F. *Angew. Chem*. **1999**, *111*, 1440. (c) Martin, R. E.; Diederich, F. *Angew. Chem., Int. Ed.* **1999**, *38*, 1350. (c) Roncali, J. *Chem. Rev.* **1997**, *97*, 173. (d) Tour, J. M. *Chem. Rev.* **1996**, *96*, 537.

(3) Moore, J. S.; Zhang, J. *Angew. Chem., Int. Ed*. **1992**, *31*, 922.

(4) Engelkamp, H.; Middelbeek, S.; Nolte, R. J. M. *Science*, **1999**, *284*, 785.

(5) Bäuerle, P. *Adv. Mater.* **1999**, *4*, 102.

(6) Hartgerink, J. D.; Clark, T. D.; Ghadiri, M. R. *Chem. Eur. J.* **1998**, *4*, 1367.

(7) Krömer, J.; Rios-Carrera, I.; Fuhrmann, G.; Musch, C.; Wunderlin, M.; Debaerdemaeker, T.; Mena-Osteritz, E.; Bäuerle, P. *Angew. Chem., Int. Ed*. **2000**, *39*, 3481.

(8) Mena-Osteritz, E.; Bäuerle, P. *Adv. Mater.* **2001**, *13*, 243.

(9) (a) Sakamoto, A.; Furukawa, Y.; Tasumi, M. *J. Phys. Chem*. **1994**, *98*, 4635. (b) Yokonuma, N.; Furukawa, Y.; Tasumi, M.; Kuroda, M.; Nakayama, J. *Chem. Phys. Lett*. **1996**, *255*, 431.

(10) Louarn, G.; Buisson, J. P.; Lefrant, S.; Fichou, D. *J. Phys. Chem*. **1995**, *99*, 11399.

(11) (a) Hernandez, V.; Ramirez, F. J.; Casado, J.; Lopez Navarrete, J. T. *J. Phys. Chem.* **1996**, *100*, 2907. (b) Casado, J.; Hernandez, V.; Hotta, S.; Lopez Navarrete, J. T. *J. Chem. Phys*. **1998**, *109*, 10419. (c) Casado, J.; Hotta, S.; Hernandez, V.; Lopez Navarrete, J. T. *J. Phys. Chem. A* **1999**, *103*, 816. (d) Hernandez, V.; Muguruma, H.; Hotta, S.; Casado, J.; Lopez Navarrete, J. T. *J. Phys. Chem. A* **2000**, *104*, 735. (e) Moreno Castro, C.; Ruiz Delgado, M. C.; Hernandez, V.; Hotta, S.; Casado, J.; Lopez Navarrete, J. T. *J. Chem. Phys*. **2002**, *116*, 10419.

(12) (a) Casado, J.; Hernandez, V.; Hotta, S.; Lopez Navarrete, J. T. *Adv. Mater*. **1998**, *10*, 1258. (b) Casado, J.; Otero, T. F.; Hotta, S.; Hernandez, V.; Ramirez, F. J.; Lopez Navarrete, J. T. *Opt. Mater*. **1998**, *9*, 82. (c) Casado, J.; Miller, L. L.; Mann, K. R.; Pappenfus, T. M.; Hernandez, V.; Lopez Navarrete, J. T. *J. Phys. Chem. B* **2002**, *106*, 3597.

(13) (a) Zerbi, G.; Castiglioni, C.; Del Zoppo, M. *Electronic Materials: The Oligomer Approach*; Müllen, K., Wegner, G., Eds.; Wiley-VCH: Weinheim, Germany, 1998. (b) Castiglioni, C.; Gussoni, M.; Lopez Navarrete, J. T.; Zerbi, G. *Solid State Commun*. **1988**, *65*, 625. (c) Hernandez, V.; Castiglioni, C.; Del Zoppo, M.; Zerbi, G. *Phys. Rev. B* **1994**, *50*, 9815. (d) Agosti, E.; Rivola, M.; Hernandez, V.; Del Zoppo, M.; Zerbi, G. *Synth. Met.* **1999**, *100*, 101.

(14) Frisch, M. J.; Trucks, G. W.; Schlegel, H. B.; Scuseria, G. E.; Robb, M. A.; Cheeseman, J. R.; Zakrzewski, V. G.; Montgomery, J. A., Jr.; Stratmann, R. E.; Burant, J. C.; Dapprich, S.; Millam, J. M.; Daniels, A. D.; Kudin, K. N.; Strain, M. C.; Farkas, O.; Tomasi, J.; Barone, V.; Cossi, M.; Cammi, R.; Mennucci, B.; Pomelli, C.; Adamo, C.; Clifford, S.; Ochterski, J.; Petersson, G. A.; Ayala, P. Y.; Cui, Q.; Morokuma, K.; Malick, D. K.; Rabuck, A. D.; Raghavachari, K.; Foresman, J. B.; Cioslowski, J.; Ortiz, J. V.; Stefanov, B. B.; Liu, G.; Liashenko, A.; Piskorz, P.; Komaromi, I.; Gomperts, R.; Martin, R. L.; Fox, D. J.; Keith, T.; Al-Laham, M. A.; Peng, C. Y.; Nanayakkara, A.; Gonzalez, C.; Challacombe, M.; Gill, P. M. W.; Johnson, B. G.; Chen, W.; Wong, M. W.; Andres, J. L.; Head-Gordon, M.; Replogle, E. S.; Pople, J. A. *Gaussian 98*, revision A.7; Gaussian, Inc.: Pittsburgh, PA, 1998.

(15) Becke, A. D. *J. Chem. Phys*. **1993**, *98*, 1372.

(16) Stephens, P. J.; Devlin, F. J.; Chabalowski, F. C. F.; Frisch, M. J. *J. Phys. Chem*. **1994**, *98*, 11623.

(17) Novoa, J. J.; Sosa, C. *J. Phys. Chem*. **1995**, *99*, 15837.

(18) Scott, A. P.; Radom, L. *J. Phys. Chem*. **1996**, *100*, 16502.

(19) Rauhut, G.; Pulay, P. *J. Phys. Chem*. **1995**, *99*, 3093.

(20) Pietro, W. J.; Francl, M. M.; Hehre, W. J.; Defrees, D. J.; Pople, J. A.; Binkley, J. S. *J. Am. Chem. Soc*. **1982**, *104*, 5039.

(21) (a) Albrecht, A. C. J. *J. Chem. Phys*. **1961**, *34*, 1476. (b) Tang, J.; Albrecht, A. C. J. *Raman Spectroscopy*; Plenum: New York, 1970.

(22) Peticolas, W. L.; Blazej, C. *Chem. Phys. Lett*., **1979**, *63*, 604.

(23) (a) Horovitz, B. *Phys. Rev. Lett*. **1981**, *47*, 1491. (b) Horovitz, B. *Solid State Commun*. **1982**, *41*, 729. (b) Ehrenfreund, E.; Vardeny, Z.; Brafman, O.; Horovitz, B. *Phys. Rev. B* **1987**, *36*, 1535.

(24) (a) Tian, B.; Zerbi, G. *J. Chem. Phys.* **1990**, *92*, 3886. (b) Tian, B.; Zerbi, G. *J. Chem. Phys.* **1990**, *92*, 3982.

(25) (a) Lopez Navarrete, J. T.; Zerbi, G. *J. Chem. Phys*. **1991**, *94*, 957. **(**b) Lopez Navarrete, J. T.; Zerbi, G. *J. Chem. Phys.* **1991**, *94*, 965.

(26) (a) Tian, B.; Zerbi, G.; Schenk, R.; Müllen, K. *J. Chem. Phys*. **1991**, *95*, 3191. (b) Tian, B.; Zerbi, G.; Müllen, K. *J. Chem. Phys.* **1991**, *95*, 3198.

(27) Hernandez, V.; Ramirez, F. J.; Zotti, G.; Lopez Navarrete, J. T. *J. Chem. Phys.* **1993**, *98*, 769.

(28) Hernandez, V.; Soto, J.; Lopez Navarrete, J. T. *Synth. Met*. **1993**, *55*−*57*, 4461,

(29) Hernandez, V.; Ramirez, F. J.; Otero, T. F.; Lopez Navarrete, J. T. *J. Chem. Phys.* **1994**, *100*, 114.

(30) Ramirez, F. J.; Hernandez, V.; Lopez Navarrete, J. T. *J. Comput. Chem*. **1994**, *15*, 405.

(31) Hernandez, V.; Berlin, A.; Zotti, G.; Lopez Navarrete, J. T. *J. Raman Spectrosc*. **1997**, *28*, 855.

(32) Casado, J.; Miller, L. L.; Mann, K. R.; Pappenfus, T. M.; Kanemitsu, Y.; Ortí, E.; Viruela, P. M.; Pou-AméRigo, R.; Hernandez, V.; Lopez Navarrete, J. T. *J. Phys. Chem. B* **2002**, *106*, 3872.

(33) Casado, J.; Pappenfus, T. M.; Miller, L. L.; Mann, K. R.; Ortí, E.; Viruela, P. M.; Pou-AméRigo, R.; Hernandez, V.; Lopez Navarrete, J. T. *J. Am. Chem. Soc*. **2003**, *125*, 2524.

(34) Hernandez, V.; Veronelli, M.; Favaretto, L.; Lopez Navarrete, J. T.; Zerbi, G. *Acta Polym.* **1996**, *47*, 62.

(35) Casado, J.; Katz, H. E.; Hernandez, V.; Lopez Navarrete, J. T. *J. Phys. Chem. B* **2002**, *106*, 2488.

(36) Ramirez, F. J.; Aranda, M. A. G.; Hernandez, V.; Casado, J.; Hotta, S.; Lopez Navarrete, J. T. *J. Chem. Phys.* **1998**, *109*, 1920.